

# PHYSICAL REVIEW B

## CONDENSED MATTER

THIRD SERIES, VOLUME 50, NUMBER 10

1 SEPTEMBER 1994-II

### X-ray-absorption studies of the $d$ -orbital occupancies of selected $4d/5d$ transition metals compounded with group-III/IV ligands

Y. Jeon

*Department of Physics, Jeonju University, Jeonju, 560-759, Korea*

J. Chen and M. Croft

*Department of Physics and Astronomy, Rutgers University, Piscataway, New Jersey 08855*

(Received 24 February 1994)

X-ray-absorption spectroscopy (XAS) is used to explore the systematic variations in the  $4d/5d$  transition-metal  $\{T = \text{Au, Pt, Ir, Re, Pd, Ag}\}$   $d$ -orbital occupancy in binary  $T$ - $X$  compounds  $\{X = \text{Al, Ga, In, Si, Ge, Sn}\}$ . Specifically, the strength of the white line (WL) feature at the  $T$ - $L_{2,3}$  edges is used to quantify the changes in the  $d$ -orbital occupancy induced by  $T$ - $X$  bond formation. Systematic chemical trends in bonding-induced  $d$ -orbital-occupancy changes, evidenced by the data, are discussed. A charge-transfer scale ( $C$  scale) is developed to approximately summarize the number of  $T$ - $d$  holes created in all of the  $T_{1-x}X_x$  compounds studied. Comparison with the electronegativity scale emphasizes that, although the  $C$  scale deals with a more restricted type of charge transfer, it provides insight into the  $T$ - $X$  bonding that is not contained in the traditional scale.

#### I. INTRODUCTION

The  $L_{2,3}$  edges of transition-metal-based materials are dominated by an intense white line (WL) feature<sup>1,2</sup> associated with the solid-state vestiges of the atomic transition into the unoccupied  $d$  states. The strength (intensity) of this transition has been used by a number of authors to estimate the number of available  $d$ -final states (i.e., the  $d$ -hole count) in  $4d$ - and  $5d$ -row transition-metal-based materials.<sup>2-8</sup> For the most part, the application of this  $L_{2,3}$ -WL method has been in isolated comparisons of  $d$ -count variations between selected pairs of compounds. These isolated studies, however, do suggest the possibility of identifying overall trends in  $d$ -orbital participation in chemical bonding. The purpose of this paper is to identify, draw together and quantify (using this WL method), patterns of transition-metal  $d$ -count variations in a systematic set of  $T$ - $X$  compounds. Specifically, intermetallic compounds involving the late transition metals  $\{T(5d) = \text{Re, Ir, Pt, and Au}; T(4d) = \text{Ag, and Pd}\}$  with the ligands  $\{X = \text{Al, Ga, In, Si, Ge, and Sn}\}$  will be addressed.

Certainly the precise role of  $d$ -orbital participation in bonding in such compounds will depend on the details of the local symmetry, ligand field strength, and other electronic structure parameters of a given compound. The spirit of this work is by no means an attempt to ignore these details but is an attempt to identify zeroth-order effects that transcend these details and depend mostly on

the atomic structure of the compound constituents. In the course of this work chemical trends are indeed observed and are noted as they arise in the discussion of the data. Finally a quantitative  $d$ -orbital charge-transfer scale, approximately summarizing all of our  $4d$  and  $5d$  compound results, is developed.

#### II. EXPERIMENTAL

##### A. Materials and spectroscopy

The compound samples were prepared by standard argon arc furnace techniques. X-ray powder-diffraction measurements (using an automated SYNTAG diffractometer) were used to verify the proper crystal structure for the various compounds and to verify the absence of impurities above the few percent level. The  $4d$  row material x-ray-absorption spectroscopy (XAS) measurements were made on beam line X-19A at the Brookhaven National Synchrotron Light Source (NSLS) using a Si(111) double-crystal monochromator. The  $5d$ -row material XAS measurements were made over a period of time at X-19A using Si(220) crystals, at the NSLS X-18B and X-23A beam lines, and at the Cornell High Energy Synchrotron Light Source. The  $4d$ -row absorption measurements were all made in the total electron yield mode to minimize finite-thickness effects.<sup>8,9</sup> The  $5d$ -row measurements were made in both the transmission and electron yield modes and again the ab-

sence of finite-thickness effects was verified. Fresh surfaces (prepared by abrasion just prior to insertion into the inert detector atmosphere) were studied in all measurements. This surface preparation and the substantial secondary electron escape depth at x-ray energies<sup>9</sup> make surface effects negligible in our studies. Extensive transition-metal oxide studies in our lab make it possible to rule out oxide feature contributions to the spectra reported here.

### B. Spectral analysis

The two most important features in the  $T$ - $L_{2,3}$  near-edge spectra are the  $d$ -hole related WL feature and the step-shaped onset of transitions to the continuum. To extract the WL feature we have relied on a method, used by a number of authors in the past,<sup>2-8</sup> to subtract off the background continuum onset. Namely, since the  $d$ -hole count and WL strength is essentially zero for the last transition-metal element in a row, the  $L_{2,3}$  edge of this element (i.e., Au for the  $5d$  row and Ag for the  $4d$  row) is used to approximate the continuum onset for spectra from that row. The steps in the WL-feature extraction procedure entail: the  $T$ - $L_1$  ( $i = 1$  or  $2$ ) spectrum and the Ag or Au background  $L_i$  spectrum are normalized so that the continuum step approaches unity at high energies (normally 50–100 eV above the edge); the elemental Ag or Au  $L_i$  spectrum is then shifted in energy so it superimposes on the other  $L_i$  spectrum in the initial 10 eV of the rise; and a difference spectra is formed by subtraction of the two.<sup>8</sup>

In Fig. 1, we illustrate the application of this method to the elemental Pd- $L_3$  spectrum. In addition to the Pd- $L_3$  spectrum, the Ag- $L_3$  background spectrum, and the Pd- $L_3$  WL-feature estimate (formed by their difference) are shown in the figure. Illustrative difference spectra are also shown in selected subsequent figures.

The WL area is calculated by integrating the difference spectrum over the WL region (i.e., between its initial rise and its first node). In some cases, where a strong fine-structure oscillation is present, the integration has been terminated before the difference spectrum has fallen to zero. Since all spectra are normalized to unity-continuum-step-height the WL-area estimates obtained in this way will have the units of eV times step height (or simply eV with the step height being implicit).

This method of WL-feature estimation has a number of potential flaws, however it has the merit of simplicity, and the capability of yielding quantitative estimates for systematic effects which are well beyond the doubt cast by the flaws. It is useful however, to keep some of the methods limitations in mind.

The use of the filled  $d$ -band elemental spectrum as a background introduces three problems. Firstly, the continuum onset in these spectra almost certainly occurs at an energy several eV higher than that implied by superimposing the background spectrum in the first 10 eV. This will produce a roughly constant error in the WL strength in all materials and should not prevent extraction of the systematics of the WL strength changes. Secondly, the nonzero but small  $d$ -hole counts of the Ag

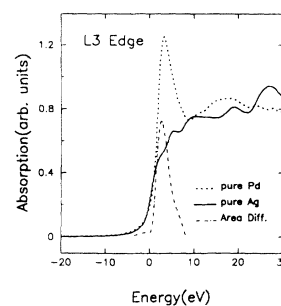


FIG. 1. The elemental Pd and Ag  $L_3$  spectra overlaid to superimpose in the initial 10 eV of the edge. The difference spectrum approximation for the  $L_3$ -WL feature of Pd is also shown.

and Au standards will contribute a systematic under estimation of the  $d$ -hole count in all compounds. Again however this should be a small effect and should not alter estimates of changes in the hole count. Thirdly, differences in fine-structure oscillations between the two spectra being subtracted will cause errors in the WL strength estimate. This effect, though clearly nonzero, is dominated by the systematics which emerge and would, at present, be impossible to compensate for.

### III. WL STRENGTH $d$ -HOLE-COUNT CONNECTION IN TRANSITION-METAL ELEMENTS

The central approximation used throughout this paper is that there is a proportionality between the  $T$ - $L_{2,3}$ -WL-area changes and the  $d$ -hole-count changes between materials.<sup>2-8</sup> Some time ago the study of Qi *et al.*<sup>2</sup> of  $5d$ -row elements showed that such a linear relationship holds between Au and W (i.e., for  $0 < \Delta h_d < 5$ ). More recently Chen *et al.*<sup>3</sup> have shown a similar approximately linear relation between the WL areas and the  $4d$  hole count in the  $4d$ -row elements Mo to Ag. The results of Chen *et al.* are reproduced in Fig. 2, where  $L_3$  results for these  $4d$  transition metals are shown. The increase in the WL-feature strength with decreasing  $4d$ -orbital occupancy between Ag and Mo is dramatically illustrated by date. (The  $L_2$  spectra, not reproduced here, manifest the

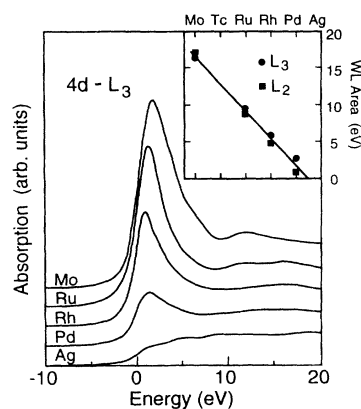


FIG. 2. The  $T$ - $L_3$  spectra of the  $4d$  transition-metal ( $T$ ) elements Mo to Ag (excluding Tc). Inset: The WL-feature areas for the  $4d$ -row elements versus atomic number (Ref. 3).

same effect.) Thus, qualitatively at least, the strong WL strength to *d*-hole-count coupling is clear.

In Fig. 2 inset we plot, versus atomic number, the integrated areas  $A_2$  and  $A_3$  of the WL features, extracted using the technique discussed in Sec. II. Note that there is an essentially linear correlation between  $A_2$ ,  $A_3$ , and atomic number between Ag and Mo. A linear least-squares fit to these data yield the average WL-area change between adjacent *4d* elements between Mo and Ag is  $3.6 \pm 0.2$  (in units of step height times eV) for both the  $L_2$  and  $L_3$  WL's.<sup>3</sup> Since band-structure calculations<sup>10</sup> indicate that the *4d*-orbital occupancy varies (on average) in very close to one-electron steps between the *4d* elements, this rate of area change can be associated with unity *d*-hole count change.

The  $L_2$  and  $L_3$  WL features separately convey information about the  $d_{3/2}$  and  $d_{5/2}$  hole counts.<sup>2,11</sup> We have, however, found that the average area ( $\bar{A}$ )

$$\bar{A} = (A_2 + A_3)/2 \quad (1)$$

is a simpler, but still meaningful parametrization for evaluating changes in the net *d* population between materials (here  $A_i$  is the  $L_i$  WL area for  $i=1, 2$ ).<sup>8</sup> The linear relations found by in the elemental studies of Qi *et al.*<sup>2</sup> and Chen *et al.*<sup>3</sup> can then be expressed as

$$\Delta h_d = (\Delta \bar{A})/a, \quad (2)$$

where  $\Delta h_d$  is the *T-d*-hole count change and  $\Delta \bar{A}$  the average WL-area change between materials.<sup>8</sup> From the *4d*-row results of Chen *et al.*<sup>3</sup> the  $a$  in (2) is given by  $a(4d) = 3.6 \pm 0.2$  in units of {(continuum step)(eV)} per *4d* hole. Similarly from the work of Qi *et al.* on the *5d* row the  $a$  in (2) is  $a(5d) = 3.0 \pm 0.02$  in units of {(continuum step)(eV)} per *5d* hole. The larger value of the *4d* row  $a$  presumably reflects the larger core-state-*d*-state dipole transition-matrix element for the more localized *4d* orbitals.

We defer the use of these quantitative hole-count/WL-area coupling until after we first discuss the qualitative WL-area variations in the range of compounds we have studied.

#### IV. RESULTS

We will proceed to discuss our *5d* and *4d* compound  $L_{2,3}$  XAS studies within the general context of the above-noted WL-area to *d*-hole count coupling. These results will be seen to naturally illustrate a number of analysis-independent observations. Specifically the relative tendencies of various ligand elements to induce transition-metal *d* holes upon compound formation will be apparent. Following this presentation we will quantitatively summarize the chemical trends from this and a previous study.<sup>8</sup>

##### A. *T(5d)-X* compounds

Motivated by a number of chemical trends noted in previous *5d* compound studies<sup>8</sup> on Al, Si, and Ge (sum-

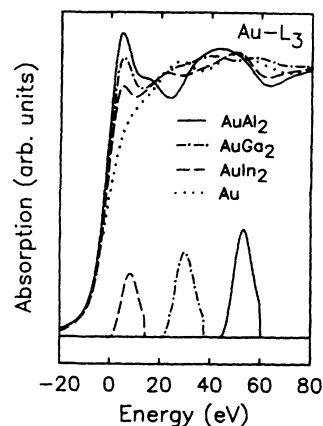


FIG. 3. The superimposed Au- $L_3$  spectra of the  $AuX_2$  compounds with  $X=Al, Ga,$  and  $In$ , along with the background elemental Au- $L_3$  spectrum. The difference spectra in the region of the WL feature are shown also.

marized later in this text) we have extended similar studies down the group III and IV rows to Ge, In, and Sn.

The first set of observations we wish to make deals with *5d* compounds involving elements from the  $X=Al, Ga,$  and  $In$  column of the periodic table. For clarity in Fig. 3, we illustrate the WL-feature extraction method for the  $L_3$  edge of these  $AuX_2$  compounds. The reference elemental Au spectrum is shown along with the WL features obtained by subtracting the reference. The termination of the WL feature to exclude a secondary fine-structure oscillation should be noted.

In Fig. 4 (left) and (right) we compare the  $L_{2,3}$  spectra of the  $TX_2$  compounds, where  $T=Au, Pt,$  and  $X=Al, Ga,$  and  $In$ . It should be noted that the strength of the *T*-WL feature in the spectra of these compounds decreases as  $X$  moves down the column from  $Al \rightarrow Ga \rightarrow In$  (see Fig. 3, also). This supports the notion that the aggressiveness of the  $X$  element in creating *T* *5d* holes, de-

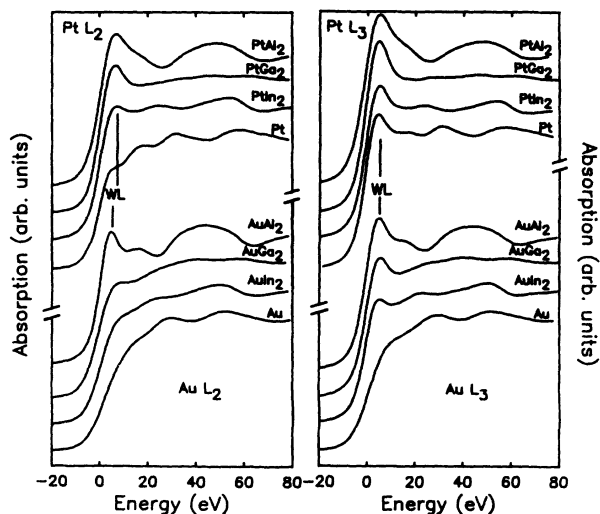


FIG. 4. The *T*- $L_2$  (left) and  $L_3$  (right) edges for the  $TX_2$  compounds with  $T=Au$  and  $Pt,$  and  $X=Al, Ga,$  and  $In$ . The elemental Au and Pt spectra are also included for comparison.

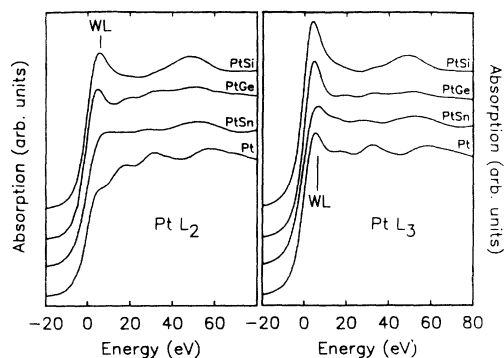


FIG. 5. The Pt- $L_2$  (left) and  $L_3$  (right) spectra of the PtX compounds with  $X = \text{Si}$ , Ge, and Sn along with the elemental Pt spectra are shown.

increases in the sequence  $\text{Al} \rightarrow \text{Ga} \rightarrow \text{In}$  (that is as the ligand varies down this column of the periodic table). It is worth noting that the electronegativity increase<sup>12</sup> from Al(1.5) to Ga(1.6) to In(1.7) qualitatively track our observed decreases of charge transfer. As we shall see below, however, the change in the degree of this charge transfer is much larger than expected based solely on electronegativity.

The second set of observations deal with  $\text{Si} \rightarrow \text{Ge} \rightarrow \text{Sn}$  column compounds. The Pt  $L_2$  and  $L_3$  edge of PtSi, PtGe, and PtSn are shown in Fig. 5. The central point we wish to note here is that the WL feature weakens progressively in the sequence  $\text{PtSi} \rightarrow \text{PtGe} \rightarrow \text{PtSn}$ . Within our interpretation, this means that the bonding-induced Pt  $5d$ -hole count goes down substantially on changing the ligand from Si to Ge to Sn (i.e., again as the ligand moves down the column in the periodic table). The strength of the  $T$ - $X$  bonding presumably tracks this  $5d$ -hole count and WL-area decrease. This last observation stands in contrast to expectations based purely on electronegativity since the electronegativity<sup>12</sup> of Si, Ge, and Sn are all identical (i.e., 1.8).

### B. $T(4d)$ - $X$ compounds

In this section we will present the results of XAS-WL studies of a number of Ag-Al, and Pd- $X$  ( $X = \text{Al}$ , Ga, In,

Si, and Sn) compounds. We will discuss first the group III compounds and then the group IV compounds.

The  $T$ - $L_{2,3}$  spectra of a series of group III compounds are presented in Figs. 6–9. Referring to the Pd-Al results in Fig. 6, the systematic increase of the WL-feature strength with increasing Al content in these compounds is clear. This trend has been observed previously in  $5d$  compounds<sup>8</sup> and will recur frequently in the  $4d$  compound results presented below.

The Ag-Al compound results in Fig. 7 evidence a similar increase in the WL area in the Al compounds (relative to pure Ag). It should be noted for later discussion that the degree of the WL-area change is substantially smaller than in the Pd-Al compounds.

The Pd-Ga spectra in Fig. 8 manifest the characteristic increase in WL area which accompanies compound formation. The degree of the WL-area increase is more modest than in the Pd-Al case. Also it is worth noting that the broadening of the compound spectra lead to an actual decrease in the peak height of the  $L_3$ -WL in the lower concentration Ga compounds.

The Pd-In  $L_3$  spectra in Fig. 9(a) dramatically extend the last point noted above, with the In compounds evidencing only decreases in the  $L_3$ -WL intensity (with respect to Pd) over the entire WL region. The  $L_2$ -WL areas of the compounds, however do show area increases relative to Pd.

The Pd- $L_{2,3}$  spectra of a series of group IV compounds are presented in Figs. 10 and 11. The  $L_3$ -WL features in both the Si and Sn compounds manifest a broadening and a decreased maximum intensity. The  $L_2$ -WL features, on the other hand, show uniform area increases relative to Pd. The greater degree of WL-area increase in the Si materials, relative to the Sn materials, is clear from the greater  $L_3$ -WL broadening and the greater  $L_2$ -WL intensities of the Si compounds.

A greater fractional area change of the Pd- $L_2$ -WL over that in the Pd- $L_3$ -WL is observed in a number of these compound series. This is presumably to the bonding-induced reduction, in the compounds, of the  $d_{5/2}$ -hole-count plurality (over the  $d_{3/2}$  holes) which is present in elemental Pd (Ref. 17). A similar relation is observed between some Pt compounds and elemental Pt,<sup>8</sup> where the spin-orbit effect also induces a  $d_{5/2}$ -state plurality near the top of the  $d$  band in the element.<sup>11</sup>

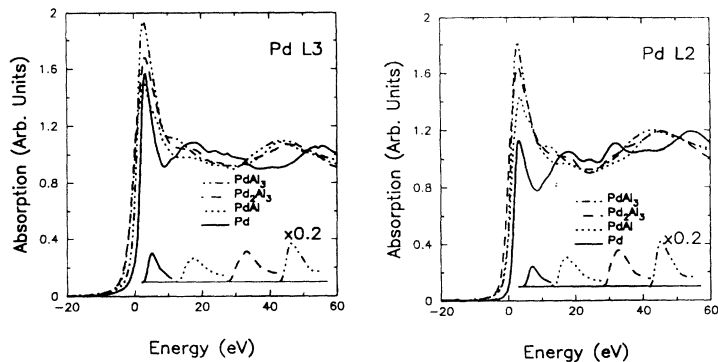


FIG. 6. The Pd- $L_3$  (left) and  $L_2$  (right) spectra of selected Pd-Al compounds along with the elemental Pd spectra are shown. The difference spectra, obtained by subtracting the Pd from the compound spectra, are also shown. The integrated area of such difference spectra are used to estimate the element to compound WL-area change and thence to estimate the  $d$ -orbital occupancy change.

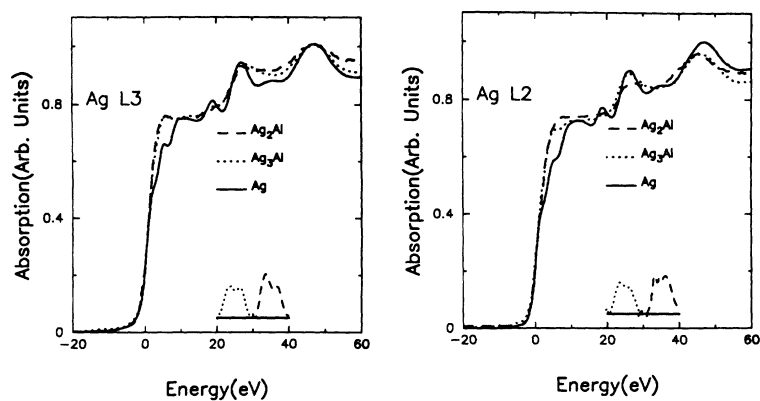


FIG. 7. The Ag- $L_3$  (left) and  $L_2$  (right) spectra of the Ag-Al compounds studied along with the elemental Ag spectra. Note that the difference spectra are also shown in the inset.

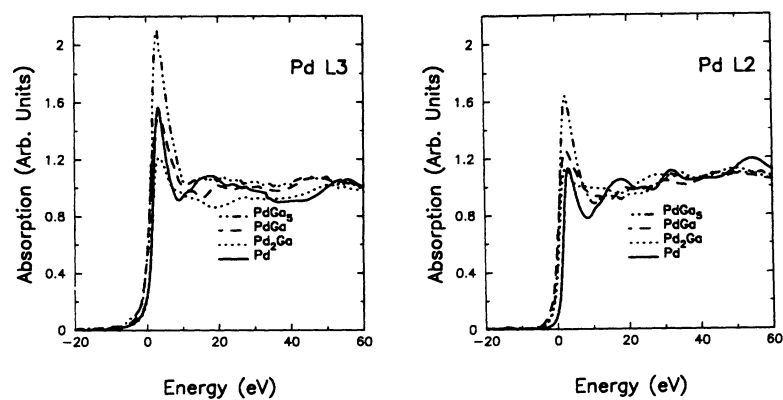


FIG. 8. The Pd- $L_3$  (left) and  $L_2$  (right) spectra of the Pd-Ga compounds studied along with the elemental Pd spectra.

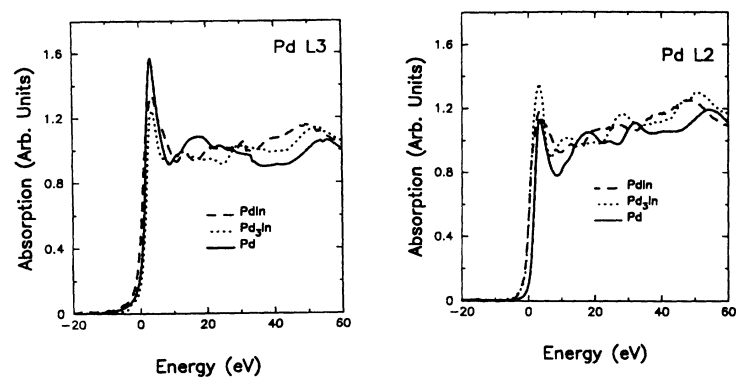


FIG. 9. The Pd- $L_3$  (left) and  $L_2$  (right) spectra of the Pd-In compounds studied along with the elemental Pd spectra.

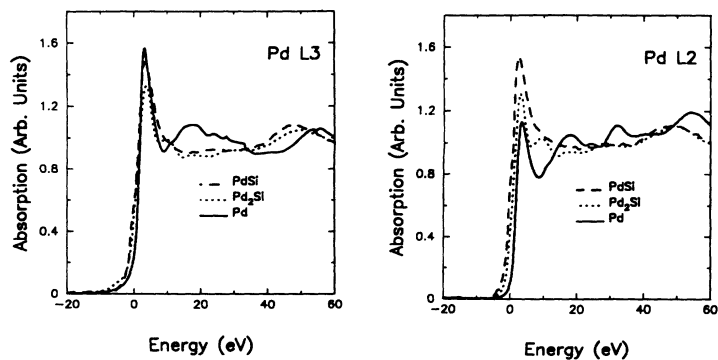


FIG. 10. The Pd- $L_3$  (left) and  $L_2$  (right) spectra of the Pd-Si compounds studied along with the elemental Pd spectra.

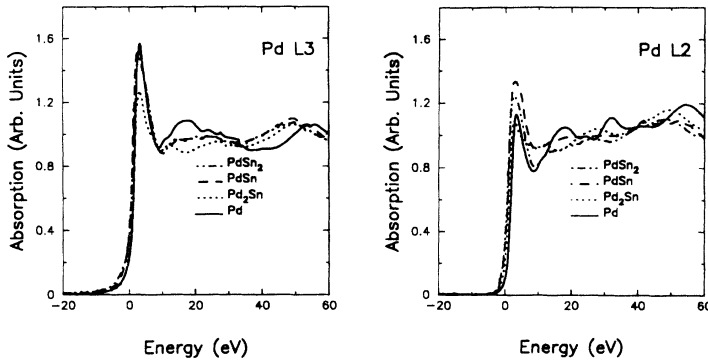


FIG. 11. The Pd- $L_3$  (left) and  $L_2$  (right) spectra of the Pd-Si compounds studied along with the elemental Pd spectra.

### V. WL-AREA VARIATIONS UPON COMPOUND FORMATION

Many authors have utilized the spirit of Eq. (2) to evaluate hole-count changes due to the bonding upon compound formation. Specifically for a  $T_{1-x}X_x$  compound one assumes that  $\Delta\bar{A}$  is now the difference in the average WL area between the element ( $x=0$ ) and the compound.<sup>8</sup> Within this approximation we will use the proportionality constants  $a(4d)$  and  $a(5d)$ , derived from the elemental studies,<sup>2,3</sup> for  $4d$  and  $5d$  compound, respectively.

The WL-feature analysis involves extracting and integrating an area of the compound WL features as described in Sec. II B; subtracting the WL area of the pure element to form the area differences due to compound formation ( $\Delta A_2$  and  $\Delta A_3$ ); and finally forming the average area change [recalling Eq. (1)]  $\Delta\bar{A} = (\Delta A_2 + \Delta A_3)/2$  to estimate the net  $d$ -hole-count changes between the element and the compound. In Fig. 12, the  $\Delta\bar{A}$  results are plotted versus  $x$  for all of the  $T_{1-x}X_x$   $4d$  compounds studied here.

Several observations should be made regarding the results plotted in Fig. 12. First, the organized increase in the bonding induced WL-area change with increasing  $x$  is clear. Second, the increasing rate of WL-area increase (with  $x$ ) in the sequences  $\text{In} \rightarrow \text{Ga} \rightarrow \text{Al}$  and  $\text{Sn} \rightarrow \text{Si}$  are also clear. Third, the much larger slope of the Pd-Al versus Ag-Al data is abundantly clear. This last point is

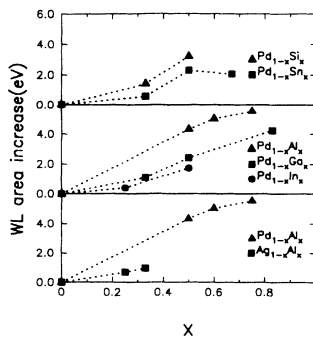


FIG. 12. The average element to compound WL-area change for the  $4d$  compounds  $T_{1-x}X_x$  ( $T = \text{Ag}$  or  $\text{Pd}$ ;  $X = \text{Al}$ ,  $\text{Ga}$ ,  $\text{In}$ ,  $\text{Si}$ , or  $\text{Sn}$ ) plotted versus  $x$ .

of some importance in ruling out  $X-p$  state contributions to the WL strength (see Ref. 18).

Previous work by our group on  $T_{1-x}X_x$  compounds<sup>8</sup> spanned various combinations of  $T = \text{Au}$ ,  $\text{Pt}$ ,  $\text{Ir}$ , and  $\text{Re}$  with  $X = \text{Al}$ ,  $\text{Si}$ , and  $\text{Ge}$ , often with several compounds of different stoichiometry ( $x$ ) in a given series. In such series (as in the  $4d$  results above) we observed a consistent increase of the WL area as  $x$  increased; and definite relations between the efficiency of  $d$ -hole creation in different chemical series. These results are emphasized by Fig. 13 (reproduced here from Ref. 8), where the  $x$  dependence of the WL-area change is shown for several series of  $T(5d)$  compounds.

To summarize the consistent increase of  $\Delta\bar{A}$  with  $x$  in a given  $T_{1-x}X_x$  series, we fit the average WL-area variation to a linear relation

$$\Delta\bar{A} = mx. \quad (3)$$

The slope  $m$  of this relation yields an average value for the rate of change of the bonding-induced WL-area changes with  $x$ . The  $\Delta\bar{A}(x)$  results in Figs. 12 and 13 have been fit to this linear relation (3) and the average slopes ( $m$ ) determined. These  $m$  values can be used to derive a charge-transfer scale (see below) to summarize the chemical systematics of these materials.

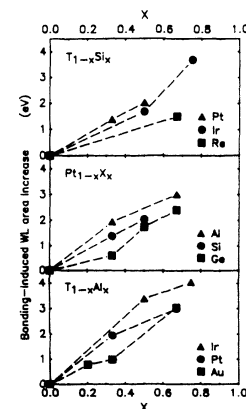


FIG. 13. (From Ref. 7.) The average bonding-induced WL-area increase for selected  $T = (\text{Au}, \text{Pt}, \text{Ir}, \text{and Re})$  compounds with  $X = (\text{Al}, \text{Si}, \text{and Ge})$ . The top set of results compares the  $T_{1-x}\text{Si}_x$  series; middle compares the  $\text{Pt}_{1-x}X_x$  series; and the bottom compares the  $T_{1-x}\text{Al}_x$  series.

VI. CHARGE-TRANSFER SCALAR *C* INDEX

**Definition:** In order to quantitatively summarize all of our results on *4d* and *5d* compounds we wish to develop a numerical scale. This charge-transfer scale (*C*-index scale) will be used to characterize the degree of charge transfer out of the *T-d* orbitals upon *T-X* compound formation. This scale has a spirit similar to electronegativity,<sup>12</sup> but addresses *d*-orbital charge changes only. We defined the charge-transfer scale (*C* index) of the *T*(*C<sub>T</sub>*) and *X*(*C<sub>X</sub>*) elements such that

$$\Delta h_d = (C_X - C_T)x \quad (4)$$

for the compound series  $T_{1-x}X_x$ . Note that the linear dependence on *x* is motivated by our previous *T*(*5d*)-*X* studies and our *T*(*4d*)-*X* studies presented above.

Using the results of the elemental studies of Qi *et al.*<sup>2</sup> for the *5d* elements [i.e.,  $\Delta \bar{A} / \Delta h_d = a(5d) = 3$ ], and of Chen *et al.*<sup>3</sup> for the *4d* elements [i.e.,  $\Delta \bar{A} / \Delta h_d = a(4d) = 3.6$ ] along with Eqs. (2), (3), and (4) one has

$$(C_X - C_T) = m/a \quad (5)$$

Substituting the slopes *m* (determined as described in the previous section) into Eq. (5), with the appropriate *a*(*5d*) or *a*(*4d*), yields the set of *C<sub>X</sub>*-*C<sub>T</sub>* equations in Table I.

**Statistical *C*-Index Determination and Uncertainties:** The over determined set of *C*-index difference equations in Table I cannot yield a unique set of *C* indices and a statistical "average approximation" set must therefore be found. We group in Table I(a) the 16 *T-X* series with *T* = Pt, Pd, Au, and Ir which have common combinations with *X* = {Al, Ga, In, Si, and Sn} and for which statistical averaging is possible. We have used an iterative computer calculation to extract a self-consistent set of average *C*-index values for these elements. Au is used as our reference so that its *C* index is assigned to zero. *C*-index estimates for Ge, Re, and Ag were determined from the equations in Table I(b) by substituting in the statistically averaged Pt, Si, and Al *C* indices. All of these *C*-index estimates are displayed in Fig. 14 in a way which is intended to emphasize their systematics as discussed below.

To estimate the statistical error of our method we have

TABLE I. The *C*-index differences from which the *C* indices were derived. (a) *T 5d* and *T 4d* results from which the self-consistent average *C* indices of *T* = Pt, Au, Ir, and Pd and *X* = Al, Ga, In, Si, and Sn were determined. (b). *T 5d* and *T 4d* results from which the *C* indexes of *T* = Ag and Re and *X* = Ge were determined.

(a)				
$C_{Al}-C_{Pt} = 1.49$	$C_{Al}-C_{Pd} = 1.90$	$C_{Al}-C_{Au} = 1.51$	$C_{Al}-C_{Ir} = 1.74$	
$C_{Ga}-C_{Pt} = 1.04$	$C_{Ga}-C_{Pd} = 1.30$	$C_{Ga}-C_{Au} = 1.11$		
$C_{In}-C_{Pt} = 0.72$	$C_{In}-C_{Pd} = 0.92$	$C_{In}-C_{Au} = 0.83$		
$C_{Si}-C_{Pt} = 1.37$	$C_{Si}-C_{Pd} = 1.78$		$C_{Si}-C_{Ir} = 1.56$	
$C_{Sn}-C_{Pt} = 0.74$	$C_{Sn}-C_{Pd} = 1.01$	$C_{Sn}-C_{Au} = 0.83$		
(b)				
$C_{Ge}-C_{Pt} = 1.22$	$C_{Si}-C_{Re} = 0.75$	$C_{Al}-C_{Ag} = 0.98$		

C index		Al	Si
		1.60 (1.5)	1.45 (1.8)
Pauling's Electronegativity		Ga	Ge
		1.10 (1.6)	1.30 (1.8)
		In	Sn
		0.80 (1.7)	0.80 (1.8)
		Pd	Ag
		-0.25 (2.2)	0.60 (1.9)
Re	Os	Ir	Pt
0.70 (1.9)		-0.10 (2.2)	0.05 (2.2)
			Au
			0.00 (2.4)

FIG. 14. A summary of the self-consistent *C* indices derived from the equations of Table I. Pauling's electronegativity values are also shown for comparison. Note that referencing the electronegativity values to Au (as the *C* scale is referenced) entails subtracting 2.4.

calculated the standard deviation of the 16 difference relations in Table I(a) with respect to the self-consistent average *C* indices. The standard deviation of these difference equations is 0.06. Using a quadratic model, this deviation for the difference equations yields a *C*-index uncertainty of  $\pm 0.04$ . Here the uncertainties of all of the *C* indices have been assumed equal.

In reporting our *C* indices we have rounded all results to the nearest 0.05 and will use the more conservative statistical uncertainty of  $\pm 0.05$ . In view of potential systematic uncertainties in the area evaluation method and the detailed  $d_{3/2}/d_{5/2}$  weighting that has been ignored we will take the still more conservative path of refraining from interpreting *C*-index differences of less than 0.10.

## VII. SUMMARY AND CONCLUSIONS

The *C* indices, shown in Fig. 14, have been constructed so as to approximately summarize all of our *T-X* XAS studies. We will therefore center our discussion on the systematic *C*-index variations. It is important to reiterate precisely the information encompassed by the *C* scale. The *C* indices represent a charge-transfer scale which specifically address electron charge transfer out of (or hole transfer into) the transition-metal *d* orbitals upon binary compound formation (between *T* = Re, Ir, Pt, Au, Ag, and Pd and *X* = Al, Ga, In, Si, Ge, and Sn). The destination to which this charge is transferred is not specified—it could involve interatomic transfer to the ligand-*X* or intra-atomic *T*-site promotion into non-*d* states.

The work of Watson and co-workers on Au and Pt compounds<sup>13-16</sup> illustrate a potential (though not necessarily the only) interpretation of the *C*-scale charge-transfer effects. Specifically for AuAl<sub>2</sub> they argued that Al-*sp* charge is transferred to the Au and an essentially equal amount (about one electron) of Au-*d* charge is back transferred to the Al.<sup>13</sup> (Here it is understood that "Al-*sp*" and "Au-*d*," respectively, refer to "*sp* symmetry as

seen from the Al site" and "*d* symmetry as seen from the Au site.") It is only the latter of these two exchanges which our XAS technique probes. Applying our *C* scale and Eq. (4) for  $\text{AuAl}_2$  (i.e.,  $\text{Au}_{1-x}\text{Al}_x$ ,  $x=0.66$ ), we find  $\Delta h_d = 1.06$ , which is the sign and the amount of *d*-orbital charge change predicted by Watson's group.<sup>13</sup> It is worth noting that since the Au site receives Au-*sp* charge and gives up Au-*d* charge in  $\text{AuAl}_2$ , it would presumably be equivalent to say that the Au-Al bonding induces promotion of Au-*d* charge into Au-*sp* states.

Before proceeding we should comment on the most common charge-transfer scale—Pauling's electronegativity.<sup>12</sup> Pauling's scale is most useful for addressing the interatomic non-*d* orbital charge transfer. In the case of  $\text{AuAl}_2$  the much larger electronegativity of Au was cited by Watson<sup>13</sup> and Pauling<sup>19</sup> as reflecting the transfer of *sp* charge into the Au-*sp* orbitals from Al. Thus on the surface it would appear that our *C* index could be used to characterize the back transfer channel of *T-d* charge to *X* thereby complementing the Pauling scale. As we shall see below however, in some cases we observe *d* orbital, *C*-index changes that vary much more than the electronegativity index.

*T Comparisons:* With the specific focus of the *C* scale in mind we will address the differing *C* indices between the transition metals. The *C* indices of Au, Pt, and Ir lie essentially within the statistical and systematic experimental uncertainties discussed earlier. Therefore our results provide an insufficient basis with which to comment on the relative susceptibilities of these three elements to form *d* holes in response to compound formation.

In contrast, the  $C_{\text{Re}} = 0.7$  value does indicate a clearly smaller degree of Re-*d* transfer upon compounding than is present in Au, Pt or Ir. In the elements these latter three elements are well beyond half filling of the *d* shell hence, (in the simplest approximation) *d*-orbital charge loss can come from the antibonding top half of the *d* band. For Re, on the other hand, such bonding-induced charge loss must come from the bonding half of the *d* band and this energy cost would be expected to dampen the *d*-charge susceptibility. Qualitatively the electronegativity decrease of Re (Ref. 12) also supports the analogous decreased degree of *sp* sphere charge transfer in Re (as compared to Au) compounds.<sup>8</sup>

Widening the discussion to the 4*d* row we will compare the *C* indices of Ag and Pd to those of Au and Pt. First we note that the *C* index for Ag is substantially larger than that of Au. The top of the elemental Ag-*d* band lies 3.4 eV below  $E_F$  whereas in elemental Au this separation is just 1.6 eV.<sup>10</sup> Thus the substantially larger susceptibility for Au-*d* hole creation in response to bonding is reasonable based on the closer proximity of the Au-*d* states to  $E_F$ .

The *C* value of  $-0.25$  for Pd stands out as the most

negative of the transition metals studied. This would indicate that Pd has the greatest propensity for *d*-orbital-hole creation (electron loss) of these *T* metals. Clearly the fact that the Fermi energy of elemental Pd lies in the *d* band, as compared to above the *d* band of Au or Ag,<sup>10</sup> supports this notion of a greater *d*-hole response for Pd. Comparing the *d*-band width of elemental Pt (7.7 eV) to that of elemental Pd (5.8 eV) it is also clear that there are more *d* states in closer proximity to  $E_F$  in Pd than in Pt.<sup>10</sup> These Pd-*d* states are therefore in a better position to hybridize with the *p* bands of the *X* elements considered here which lie mostly at and above  $E_F$ . Thus a stronger *T-X* hybridization (and hence a larger antibonding *d*-state transfer above the compound  $E_F$ ) is not unreasonable for Pd as compared to Pt.

Again, it is worth making contact with the electronegativity scale to highlight the insight gained from the *C* scale. Comparing the electronegativities of Ag and Au indicates a smaller chemical activity of Ag in the *sp*-charge-transfer channel, which is similar to the *d*-channel *C*-index prediction. (Recall of course that the direction of the charge transfer is opposite in the two channels). On the other hand the electronegativity of Pd is the same as Pt and less than that of Au. This stands in contrast to our observation that Pd has a greater tendency to lose *d*-orbital charge than either Pt or Au.

*X Comparisons:* It is between the *X*-ligand elements as one moves down a column of the periodic table that the clearest *C*-index trends emerge. Specifically there is a consistent *C*-index decrease in the Al→Ga→In and Si→Ge→Sn sequences. This presumably indicates a decreasing tendency for the *T-X* bonding to shift antibonding *T-d* states above  $E_F$  in these sequences. Certainly in the Si→Ge→Sn sequence the constant electronegativity gives no indication of a change in *sp*-orbital chemical activity.<sup>12</sup> In the Al→Ga→In sequence only a small *sp*-channel activity change is supported by the small electronegativity change.<sup>12</sup> By contrast a dramatic *T-d*-channel activity change, in compounds from this sequence, is indicated by the large *C*-index change as *X* varies from Al→Ga→In.

*Closing:* The *C*-scale results (constructed from our XAS studies) points to some potentially very basic themes in *T(d)-X(sp)* bonding in the solid state. Often theoretical band-structure calculations obscure such basic themes in the myriad details of their predictions. Critical theoretical electronic-structure discussion of these more general ideas would be highly useful.

#### ACKNOWLEDGMENTS

Travel to NSLS for Y. Jeon was funded by the user program of the Polang Light Source.

<sup>1</sup>G. Materlik, J. E. Muller, and J. W. Wilkins, Phys. Rev. Lett. **50**, 267 (1983).

<sup>2</sup>Boyun Qi, I. Perez, P. H. Ansari, F. Lu, and M. Croft, Phys. Rev. B **36**, 2972 (1987), and references therein.

<sup>3</sup>J. Chen, M. Croft, Y. Jeon, X. Xu, S. Shaheen, and F. Lu, Phys. Rev. B **46**, 15 639 (1992).

<sup>4</sup>F. Lytle, J. Catal. **43**, 376 (1976).

<sup>5</sup>I. Perez, B. Qi, G. Liang, F. Lu, M. Croft, and D. Wieliczka,



- Phys. Rev. B **38**, 12 233 (1988).
- <sup>6</sup>A. N. Mansour, J. W. Cook, Jr., and D. E. Sayers, J. Phys. Chem. **88**, 2330 (1984).
- <sup>7</sup>T. K. Sham, Solid State Commun. **64**, 1103 (1987).
- <sup>8</sup>Y. Jeon, B. Qi, F. Lu, and M. Croft, Phys. Rev. B **40**, 1538 (1989).
- <sup>9</sup>T. Guo and M. denBoer, Phys. Rev. B **31**, 6233 (1985).
- <sup>10</sup>D. Papaconstantopoulos, *Handbook of the Bandstructure of Elemental Solids* (Plenum, New York, 1986).
- <sup>11</sup>L. F. Mattheiss and R. E. Dietz, Phys. Rev. B **22**, 1663 (1980).
- <sup>12</sup>L. Pauling, *The Nature of the Chemical Bond* (Cornell University Press, New York, 1960), p. 93.
- <sup>13</sup>R. E. Watson, J. Hudis, and M. L. Pearlman, Phys. Rev. B **4**, 4139 (1971).
- <sup>14</sup>T. K. Sham, M. L. Perlman, and R. E. Watson, Phys. Rev. B **19**, 539 (1979).
- <sup>15</sup>T. S. Chou, M. L. Perlman, and R. E. Watson, Phys. Rev. B **14**, 3248 (1976).
- <sup>16</sup>R. E. Watson, J. W. Davenport, and M. Weinert, Phys. Rev. B **35**, 508 (1987).
- <sup>17</sup>N. E. Christensen, J. Phys. F **8**, L51 (1978).
- <sup>18</sup>Specifically if the WL-area changes were due to crossover transitions from the *T-2p* states into the *X-p* states above  $E_F$  then one would expect similar area changes (at the same  $x$  value) in both Ag and Pd compounds. The much smaller tendency of the Ag compounds to show WL-area changes supports the proposed association of these area changes with *T d*-orbital-occupancy changes. Namely the Ag-4*d* orbitals lie further below the Fermi energy (than those of Pd which cross  $E_F$ ) (Ref. 10), and hence their susceptibility to being transferred above  $E_F$  is reduced with respect to Pd.
- <sup>19</sup>L. Pauling, *The Nature of the Chemical Bond* (Ref. 12), p. 431.